Prediction of Rocket Exhaust Flowfields

ROGER J. REIS,* PAT J. AUCOIN,† AND R. CARL STECHMAN‡
The Marquardt Company, CCI Corporation, Van Nuys, Calif.

A numerical method has been developed for determining the flowfield characteristics of a rocket exhaust plume. It employs the method of characteristics and includes the effects of the nozzle boundary layer, coalescence shock, and nonisentropic flow. Analytical procedures are used which result in elimination of many of the time-consuming numerical procedures previously associated with the solution of the characteristic equations for a rotational flowfield. Comparisons of the computed results with test data obtained from various sources indicate this method will accurately predict the flowfield of a rocket engine exhaust. A 1-lb-thrust, monopropellant rocket plume boundary calculated by this method, including the effect of the nozzle boundary layer, showed good agreement with the experimentally determined boundary.

Nomenclature

a	=	local speed of sound
c_p	=	specific heat at constant pressure
c_v	=	specific heat at constant volume
M	=	Mach number
m	=	molecular weight, slope
P	=	pressure
q	=	$(u^2 + v^2)^{1/2}$
R	=	universal gas constant
S	=	entropy
T	=	temperature
u,v	=	velocity
y,x	=	coordinates in x-y space
γ	=	ratio of specific heats
δ	=	angle between entering and exit streamline
ϵ	=	0 for two-dimensional case, 1 for axisymmetrical case
η	=	$\perp$ to streamline direction
θ	=	flow angle (measured counter clockwise from X axis)
ξ	=	streamline direction
ρ	=	density
σ	=	angle of inclination of the shock entering streamline

Subscripts

i,j	=	local conditions
T	=	total conditions
US,DS	=	upstream, downstream
SR	=	streamline intersect

Introduction

THE expansion of an underexpanded rocket exhaust plume (Fig. 1) is determined by the difference between the static pressure at the nozzle exit and the ambient static pressure. For exhaust into the near absolute vacuum in space even the vapor pressure of the propellants will cause large expansive plumes, which may interact with the vehicle, introducing aerodynamic forces and heat-transfer effects. Degradation of the vehicle surface may result, and the plume may cause electrostatic and electromagnetic radiation effects, including the attenuation of radio signals and reflection of radar signals. Finally, during pulse operations the residual propellants emptying from the injector after each firing can be entrained and blown out with the exhaust products. These effects must be taken into account during the design of the vehicle. An accurate representation of the plume flowfield is required. Plume flowfields may be divided into two general categories: "vacuum plumes" and "high-altitude plumes."

Analytically, the vacuum plume consists of several distinct regions. The first region is between the nozzle exit and the last $2D$ or Prandtl-Meyer expansion wave. This region is isentropic if the initial flow is isentropic and contains the Prandtl-Meyer turning region. Further downstream, the field contains waves reflected from the boundary. These reflected waves become more inclined and coalesce into a shock wave (Fig. 1), which is caused by the curvature of the boundary. As the boundary curves, the shock becomes stronger and eventually results in a shock triple point with the resulting formation of a Mach disk. The flow behind the Mach disk is subsonic and essentially a turbulent wake. The flow between the coalescent shock and the boundary is rotational.

For rocket engines with boundary layers and film cooling, the flow entrained outside of the central core within the nozzle can amount to 20% or more of the total flow. The initial conditions at the nozzle exit cannot be assumed isentropic, and the entire plume field is rotational. The lower exit Mach number near the walls of the nozzle will result in a higher initial turning angle and a more expansive plume. Condensation shocks or shocks associated with "Rao" type nozzles will also reduce the exit Mach number and increase the initial expansion.

High-altitude plume acts as a large blunt body and creates a flowfield much like a re-entry vehicle (Fig. 2). The plume contains a mixing zone between the rocket gases and the ambient air in the initial blunt-body bow shock. This combined flowfield may be determined by first calculating the

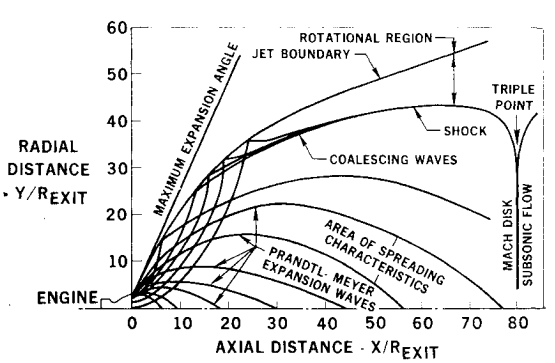

Fig. 1 Typical rocket exhaust plume.

Presented as Paper 69-569 at the AIAA 5th Propulsion Joint Specialist Conference, U.S. Air Force Academy, Colo., June 9–13, 1969; submitted June 9, 1969; revision received October 16, 1969.

* Member of the Advanced Technical Staff, Rocket Systems Division.

† Special Member of the Advanced Technical Staff, APL Computing Services Division.

‡ Manager, Development Engineering, Propulsion Division. Member AIAA.

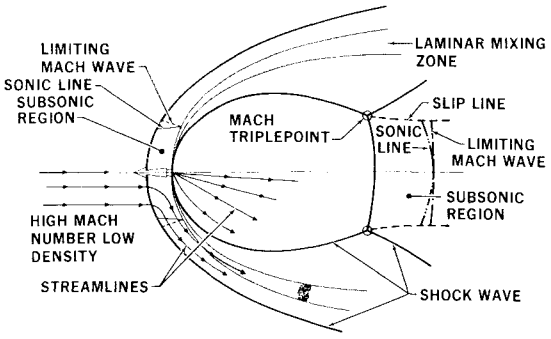

Fig. 2 Typical high-altitude plume flowfield.

"vacuum" plume for some constant finite back pressure. For an initial approximation the pressure behind a hypersonic normal shock at the vehicle conditions would be used. The resulting plume would then be used as a blunt-body profile to calculate the shape of the bow shock, and the Newtonian surface pressure. This pressure profile is then used to recalculate the "vacuum" plume and the process is repeated until the process converges. The mixing zone is calculated using standard boundary-layer theory. Napolitano[1] has shown good results for plumes at lower altitudes using this method. The interaction of the hypersonic bow shock and mixing layer does not materially alter the shape near the vehicle of the "vacuum" plume generated at some back pressure related to the Newtonian pressure distribution. For the case of local vehicle impingement, the detailed calculation described previously need not be carried out.

Flowfield Determination

The problem relative to calculating the "vacuum" plume flowfield is whether or not the continuum flow equations will describe the flow. The Knudsen number (the ratio of the mean free path to some characteristic length) is used as the indicator of the flow regime. Free molecular flow is defined as the region where the Knudsen number is greater than 10. For Knudsen numbers between 10 and 0.01 the flow is in a region not clearly understood, and is referred to as the transition regime. Boundary-layer calculations and other surface calculations may not be valid in this region due to the slip effect of the molecules relative to the surface in question. Koga,[2] using the Chapman-Enskog method to derive the Navier-Stokes equations from the Boltzmann equation, indicates that the Navier-Stokes equations are valid in this region. Thus, the continuum equation would be valid in the plume field for values of the Knudsen number near 1. Using the plume diameter as the reference length, calculations have been made to evaluate the Knudsen number for typical flowfields. Probstein[3] showed the free molecular flow region for a 2-ft-diam re-entry sphere to be above 90 miles. The maximum plume diameter may be in the order of 800 nozzle diameters, or more for high-altitude plumes. Thus, the use of the continuum flow equations can be considered valid.

Using Ref. 3 to ascertain mean free path and Vick[4] to estimate maximum boundary radius, typical Knudsen numbers for a 100-lb-thrust rocket engine are shown in Table 1. As shown, no difficulty would be expected with the use of the continuum equation for the determination of space plumes. Work done by Yoshihara,[5] Koga,[2] and Cassanova et al.[6] further bear out these assumptions. References 1 and 7 included calculations of plume flowfields with large boundary Mach numbers and showed the validity of the continuum calculations. The continued validity of the continuum calculations at higher and higher Mach numbers is the result of the flow approximating pure source flow in the far field. The expression for the zone of influence in the continuum flow reaction is $\sin^{-1}(a/u)$, where u is the flow speed, and a is the local speed of sound, $(\gamma RT/m)^{1/2}$. For the kinetic case, the expression is $\sin^{-1}(u_i/u)$, where u is again the flow speed, and (u_i) is the local molecular speed $(8RT/\pi m)^{1/2}$. The expressions are almost identical, except for the constant. It is of interest to note that the value of γ will vary as various energy modes reach equilibrium or freeze at a given temperature. This no doubt explains the smooth transition from continuum flow to free molecular flow.

Two general methods are used for describing plume fields. The first uses a source flow solution with some form of perturbation series to describe the flowfield. This method yields adequate results in the far field but suffers from lack of detail in the near field where impingement is likely. As with all approximate solutions, an excessive number of terms may be required for accurate determination of the field. These methods are based on the irrotational flow assumptions and thus do not accurately describe the embedded shock due to boundary curvature or the nonisentropic nature of the nozzle exhaust gases. The second method for the determination of flowfields is the method of characteristics. Love et al.[7] Vick et al.,[4] and Cassanova et al.[6] have presented irrotational methods of characteristics to calculate plumes. They use various methods for handling the numerical difficulties near the axis and for handling the crossing of characteristic lines of the same family resulting from the coalescence shock. However, these methods do not accurately represent the coalescence shock, predict the location of the shock triple point, or handle nonisentropic starting lines. The method of characteristics is an exact solution to the nonlinear set of differential equations describing the flow. It results in high resolution and detail in the near field for cases where the starting line is nearly isentropic as is the case for reasonably large well designed nozzles using air. Vick et al.[4] show many schlieren photos superimposed with calculated boundaries; a loss in accuracy can be seen at points downstream where the shock has gained appreciable strength.

Since the methods of characteristics gives good results, with the exception noted previously, a method-of-characteristics computer program which incorporates the properties of a rotational flowfield and changing chemical composition was developed.

Analytical Methods

The principal advantages of the procedures developed are: 1) the method of characteristics provides an accurate solution with high resolution in the near flowfield, 2) the rotational nature of the procedure allows calculation of the embedded shocks, 3) the initial condition may be nonisentropic, 4) the effect of chemical equilibrium (in terms of variable gamma) may be included, and 5) the procedures provide an optimum computer program in terms of accuracy and calculation time, while containing few areas of complex numerical methods.

Finite-Difference Equations for Characteristics of Nonisentropic Irrotational Flow—No shocks

The plume flowfield is calculated by applying the following finite-difference equations (derived from the flow equation characteristics, Shapiro[8]) to the points $i + 1$ and i where flow

Table 1 Typical Knudsen numbers for high-altitude plumes

P_{exit}/P_0	Altitude	Nozzle Exit radius, in.	Knudsen number
157,895	300,000 ft	3.0	2.6×10^{-4}
2×10^7	150 miles	3.0	1

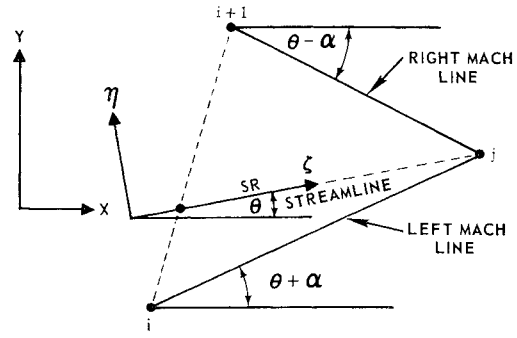

Fig. 3 Characteristics network.

characteristics are known;

$$y_j - y_i = (x_j - x_i)\tan\tfrac{1}{2}(\theta_i + \alpha_i + \theta_j + \alpha_j) \quad (1)$$

$$y_j - y_{i+1} = (x_j - x_{i+1})\tan\tfrac{1}{2}(\theta_{i+1} - \alpha_{i+1} + \theta_j - \alpha_j) \quad (2)$$

$$\tan\alpha = (M^2 - 1)^{-0.5} \quad (3)$$

$$x_{SR} = (y_j - y_i + mx_i - x_j\tan\theta_j)/(m - \tan\theta_j) \quad (4)$$

$$y_{SR} = x_{SR}\tan\theta_j + y_j - x_j\tan\theta_j \quad (5)$$

$$m = (y_{i+1} - y_i)/(x_{i+1} - x_i) \quad (6)$$

$$\frac{4[(M_i + M_j)^2 - 4]^{0.5}(P_j - P_i)}{(q_i + q_j)^2(\rho_i + \rho_j)} + (\theta_j - \theta_i) + \frac{4\epsilon\sin\tfrac{1}{2}(\theta_i + \theta_j)[(x_j - x_i)^2 + (y_j - y_i)^2]^{0.5}}{(y_i + y_j)(M_i + M_j)} = 0 \quad (7)$$

$$\frac{4[(M_{i+1} + M_j)^2 - 4]^{0.5}(P_j - P_{i+1})}{(q_{i+1} + q_j)^2(\rho_{i+1} + \rho_j)} - (\theta_j - \theta_{i+1}) + \frac{4\epsilon\sin\tfrac{1}{2}(\theta_{i+1} + \theta_j)[(x_j - x_{i+1})^2 - (y_j - y_{i+1})^2]^{0.5}}{(y_{i+1} + y_j)(M_{i+1} + M_j)} = 0 \quad (8)$$

$$0.25(q_j + q_{SR})(\rho_j + \rho_{SR})(q_j - q_{SR}) + (P_j - P_{SR}) = 0 \quad (9)$$

$$\frac{\gamma(T_j + T_{SR})}{2}\left(\frac{P_j + P_{SR}}{\rho_j + \rho_{SR}}\right)(\rho_j - \rho_{SR}) - (\rho_j - P_{SR}) = 0 \quad (10)$$

$$P = \rho RT \quad (11)$$

These equations are solved to determine the location and properties of point j as shown in Fig. 3. (The properties at SR can be obtained by linear interpolation from those at points i and $i + 1$.) Equation (1) represents the left Mach line; Eq. (2), the right Mach line. Equation (7) is the compatibility equation corresponding to the left Mach line, and Eq. (8) corresponds to the right line. Equations (9) and (10) hold along the streamline.

Shock Equations

The method of characteristics does not accurately represent the flowfield in the neighborhood of a shock; the computer program detects a shock by testing successive iterations. When coalescence is detected, the program constructs the shock based on the following equations:

$$\rho_{US}q_{US}\sin\sigma = \rho_{DS}q_{DS}\sin(\sigma - \delta) \quad (12)$$

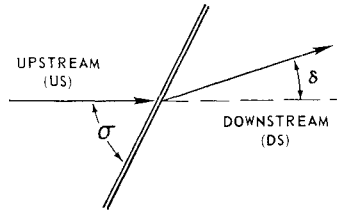

Fig. 4 Shock network.

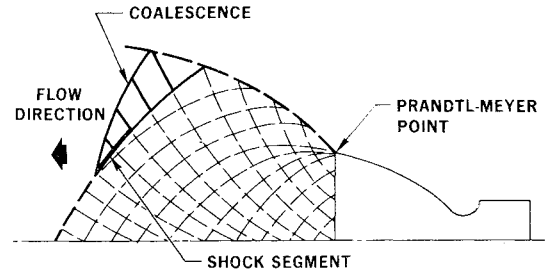

Fig. 5 Flowfield construction.

$$q_{US}\cos\sigma = q_{DS}\cos(\sigma - \delta) \quad (13)$$

$$P_{US} - \rho_{DS} = \rho_{DS}q_{DS}^2\sin^2(\sigma - \delta) - \rho_{US}q_{US}^2\sin\sigma \quad (14)$$

$$2\int_{T_{DS}}^{T_{US}} c_p(T)dT = q_{DS}^2 - q_{US}^2 \quad (15)$$

If $c_p(T)$ is assumed to be a linear function of temperature across the shock, Eq. (15) can be replaced by

$$2c_{pav}(T_{US} - T_{DS}) = q_{DS}^2 - q_{US}^2 \quad (15')$$

where c_{pav} is the specific heat at the mean temperature across the shock, $(T_{US} + T_{DS})/2$. These equations represent the shock as shown in Fig. 4. (Note that $\theta_{DS} = \theta_{US} + \delta$.)

The shock equations and finite-difference characteristic functions completely describe the flowfield; when the characteristic functions become discontinuous at a shock, the shock equation calculates the properties upstream of the shock. [For weak shocks—$(P_{US} - P_{DS})/P_{DS} \ll 1$, i.e., isentropic—the equations simplify and a table of T vs M vs P/P_t vs q is used to reduce solution time.]

Calculation Procedure and Program Features

The computer program generates the exhaust flowfield in the following manner (see Fig. 5).

1) If the initial line is not a left line, a starting left line is constructed from the initial line data. The construction is based on successive intersections of left- and right-line segments.

2) The Prandtl-Meyer flow region, consisting of a fan of left lines originating at the Prandtl-Mayer point, is constructed. Every Nth left line is stored for future use as part of the upstream flowfield in the shock construction to follow, where N is an input (typically equal to 3 or 4). If it is anticipated that the shock will not invade the Prandtl-Meyer region, N can be set to a large number such as 30 or 40.

3) The jet streamline is constructed by intersecting the jet streamline segment with a right-line segment until the external pressure field bends it back enough to cause left-line coalescence. Every NJth left line is stored (NJ input). The coalescence is determined and the point of coalescence is

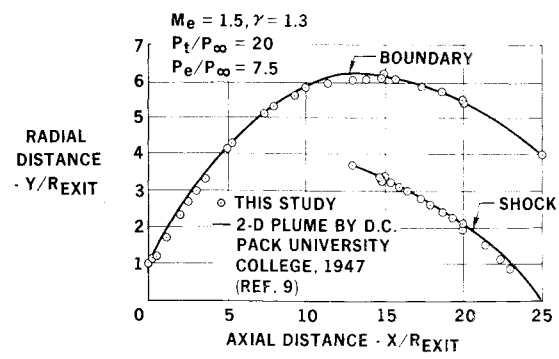

Fig. 6 Two-dimensional plume, comparison of analytical methods.

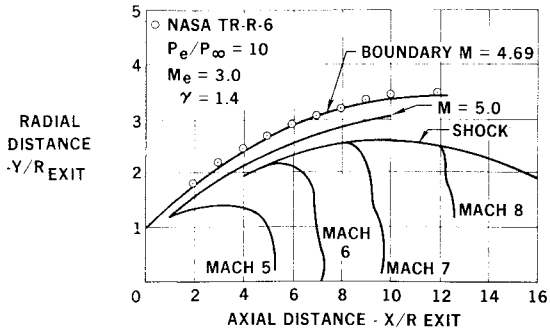

Fig. 7 Axisymmetrical flowfield, comparison of jet boundaries.

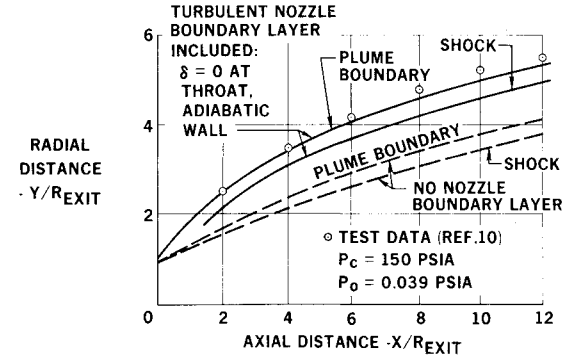

Fig. 9 Comparison of plume boundary with and without nozzle boundary layer.

the beginning of the shock. At this point the shock has zero strength.

4) The shock is then constructed. Each successive left line from now on, beginning at the jet streamline, will end on a shock segment.

The program can analyze two-dimensional or axisymmetric flow. The Prandtl-Meyer turning is set up so that the left lines in the fan are uniformly spread; this is done by making ΔP decrease as P decreases. If an error occurs in an arithmetic subroutine, a new point is inserted in the previous left line, and the current line is recalculated. If an error then occurs at the same index number, a first-order correction technique is used to insure reasonable results. These actions are displayed in the output. The point addition is used to compensate where necessary for the line spreading troubles associated with axisymmetric plume calculations. When a shock segment is built, a new point is added if the shock segment is relatively longer than the spreading of adjacent Mach line segments. The density of information for the upstream flowfield storage is under user control. A considerable reduction in run time is possible if the initial line is isentropic. Also, the relative numerical error level is under user control. The flowfield may be truncated along a right line reflected from the centerline or at a fixed value of x, downstream. For right-line truncation both these features may be used yielding a flowfield shaped as below. This reduces the problem of net spreading far downstream near the centerline and decreases run time.

Results

Figure 6 shows the excellent agreement between results obtained from the computer solution and those calculated by the method of characteristics[9] for the case of a two-dimensional plume.

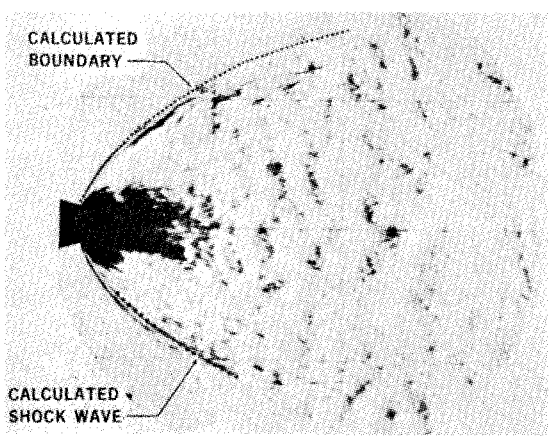

Fig. 8 Axisymmetrical plume flowfield, comparison of schlieren with analytical results.

Results for various axisymmetrical flowfields were compared to those of other studies. A comparison was made with a plume boundary presented by Love[7] (Fig. 7). Again, the excellent agreement indicates the validity of the procedures. Computed features are compared with those in a schlieren photograph of a high-altitude plume from the work of Vick et al.[4] in Fig. 8. The excellent agreement for both the boundary and the embedded shock in this figure is due to the exact solution provided by the rotational equation in the region of the shock and boundary.

The analytical methods were used to generate a plume for a 1-lb-thrust, monopropellant rocket engine. Due to the small size of the nozzle, the boundary layer was expected to affect the size and shape of the plume. The plume was generated both considering the effect of the boundary layer and without considering the boundary layer. The results (Fig. 9) were compared with tests conducted in a Marquardt vacuum test facility.[10] The results clearly define the jet boundary and shock. The agreement of the jet boundary, which includes boundary-layer flow with the experimental plume, indicates the significance of the boundary-layer flow in the determination of the plume flowfields for small rocket engines. This particular plume was determined with relative ease when compared to the previous methods which required a significant amount of computer time.

Conclusions

A numerical method was developed which accurately determines the rocket exhaust flowfield and can include the effects due to boundary layer, shock waves, and nonisentropic flow. The computer program includes analytical procedures which eliminate the time-consuming procedures previously associated with the solution of the characteristic equation for a rotational flowfield. Comparisons of computed results with test data indicate that this new technique provides accurate predictions.

References

[1] Napolitano, L. G., "Critical Study of the Academy of Integral Methods in Plane Mixing Problems," PIBAL Rept. 425, (AD 136 746), Dec. 1957, Polytechnique Institute of Brooklyn, New York.

[2] Koga, T., "Dynamic Similarities in Rarefied Gas Flows," PIBAL Rept. 964, Jan. 1966, Polytechnic Institute of Brooklyn, New York.

[3] Probstein, R. F., "Shock Wave and Flow Field Development in Hypersonic Re-entry," *Journal of the American Rocket Society*, Vol. 31, No. 2, Feb. 1961.

[4] Vick, A. R. et al., "Comparisons of Experimental Free Jet Boundaries with Theoretical Results Obtained with the Method of Characteristics," TN D-2327, 1964, NASA.

[5] Yoshihara, H., "Gasdynamics of Rocket Exhaust Plumes," Rept. A-63-1381, Dec. 1963, General Dynamics/Astronautics.

[6] Cassanova, R. A., "Expansion of a Jet into a Vacuum," *Eleventh International Symposium on Combustion*, Univ. of California, Berkeley, Calif., 1966.
[7] Love, I. S. et al., "Experimental and Theoretical Studies of Axisymmetric Free Jets," TR-R-6, 1959, NASA.
[8] Shapiro, A. H., *The Dynamics and Thermodynamics of Compressible Flow*, Vols. I and II, Roland Press, New York, 1953.
[9] Pack, D. C., "On the Formation of Shock Waves in Supersonic Gas Jets," 1947, Univ. College, Dundee, Scotland.
[10] Stechman, R. C. et al., "Hydrazine Monopropellant Rocket Engine Plume Tests," Internal Report 79, June 1967, Rocket Systems Div., The Marquardt Corp., Van Nuys, Calif.

FEBRUARY 1970 J. SPACECRAFT VOL. 7, NO. 2

Swirling Flow through a Nozzle

JAMES L. BATSON*
U.S. Army Missile Command, Redstone Arsenal, Ala.
AND
RICHARD H. SFORZINI†
Auburn University, Auburn, Ala.

This paper presents the results of an experimental investigation of swirling flow through a nozzle. Its purpose is to determine the effect of swirl on the flowfield, thrust and mass flow produced by nozzled devices. Swirling flow is induced by injecting cold gas tangentially to a cylindrical chamber wall. The internal flow characteristics are determined by use of miniature probes. Liquid injection provides a means of flow visualization. Nozzle exhaust flow is examined by a shadowgraph. Thrust and mass flow rates are obtained for four swirl conditions and related to axial flow theory and to Mager's solution of isentropic swirling flow. The results have implications with respect to performance of spinning rocket motors.

Nomenclature

a_o = total speed of sound
M, M_I = mass flow and axial isentropic mass flow
P_C, P_{OC} = static and stagnation pressures in the chamber
P_O = stagnation pressure of inlet flow
R = radius of cylindrical chamber
r = radius of position in flowfield
r_C = radius of exhaust core measured at exit plane
r_e = radius of nozzle exit
r^* = radius of nozzle throat
T_C, T_{OC} = static and stagnation temperatures in the chamber
T_O = stagnation temperature of inlet flow
V = tangential velocity in the chamber near the wall at station 2
v = tangential velocity
α^* = Mager's swirl parameter $= RV[(\gamma - 1)/2]^{1/2}/r^* a_o$
γ = ratio of specific heats (for air = 1.4)
ρ_c = static density in the chamber
ρ_o = stagnation density of inlet flow

Introduction

SWIRLING flow occurs in many rockets (especially spin-stabilized rockets), jet engines, plasma jets (to stabilize the arc), vortex valves, industrial furnaces (vortex burners), and cyclone separators. Despite the interest created by these applications, the mechanics of swirling flow are not clearly understood, especially with respect to the passage of the flow through a nozzle.

Spin produces swirling flow within a solid-propellant rocket motor (SRM) by imparting angular momentum to the gas evolving from the surface of the burning grain. Because of the conservation of angular momentum, the swirling motion becomes very intense in the nozzle throat, as does the motion of a spinning ice skater who brings his arms down to increase his spin. The axial movement of the gas is impaired, so that the effective throat area is reduced. The chamber pressure will tend to increase because of the inability of the nozzle to pass the mass generated in the SRM at a lower pressure, resulting in a higher burning rate and, to satisfy continuity relations, in a new and higher equilibrium operating pressure. The action of swirling flow on the burning surface of the propellant can cause grain erosion aggravating the situation. These events coupled with the effect of centrifugal force on the combustion mechanism of the propellant may cause the chamber pressure to exceed the structural limits of the motor case, ending in catastrophic failure. In a liquid-propellant rocket the effective throat constriction can also result in significant changes in operating conditions, unless a control system compensates for it.

To date, little information has been published on measured effects of swirl upon mass flow and thrust. It is impractical to probe the flow within an SRM rotating at 3000 to 20,000 rpm, and it is difficult to isolate the effect of swirling flow through the nozzle. The method of inducing swirl used in this research was injection of cold gas tangentially to a cylindrical chamber wall as in the vortex or Ranque-Hilsch tube.[1-5] This method of producing swirl was advantageous in that no moving parts were required, thus facilitating the measurement of the internal flowfield. Although the properties of cold gas do not match the properties of the hot gas in a rocket, and the character of the energy equation differs between cold and hot gas, the results provide a means for basic understanding of swirling flow.

The nature of the vortex formed within the Ranque-Hilsch tube is that of a free or potential vortex. One would also expect this type of flow to be a characteristic of the flow within an internal-burning SRM. The spinning of the propellant surface in an SRM imparts a tangential velocity to the flow, whereas in the experimental apparatus the flow

Received June 9, 1969; revision received October 3, 1969. This research was conducted at Auburn University in conjunction with the Master of Science in Aerospace Engineering program of J. L. Batson.
* General Engineer (Missiles), Research and Engineering Directorate; presently a graduate student in aerospace engineering at the University of Texas. Member AIAA.
† Professor of Aerospace Engineering. Member AIAA.